Dense arrays of site-controlled quantum dots with tailored emission wavelength: Growth mechanisms and optical properties

Article *in* Applied Physics Letters · November 2017

DOI: 10.1063/1.5004407

CITATIONS
11

READS
126

6 authors, including:

Alessandro Surrente
Wroclaw University of Science and Technology
60 PUBLICATIONS **1,654** CITATIONS
SEE PROFILE

Marco Felici
Sapienza University of Rome
99 PUBLICATIONS **1,490** CITATIONS
SEE PROFILE

Pascal Gallo
LakeDiamond SA
68 PUBLICATIONS **1,227** CITATIONS
SEE PROFILE

E. Kapon
École Polytechnique Fédérale de Lausanne
700 PUBLICATIONS **14,109** CITATIONS
SEE PROFILE

Dense arrays of site-controlled quantum dots with tailored emission wavelength: growth mechanisms and optical properties

Alessandro Surrente,[1] Marco Felici,[1, a)] Pascal Gallo,[1] Alok Rudra,[1] Benjamin Dwir,[1] and Eli Kapon[1, b)]
Laboratory of Physics of Nanostructures, École Polytechnique Fédérale de Lausanne, CH-1015 Lausanne, Switzerland

(Dated: November 16, 2017)

We demonstrate the fabrication of arrayed, site-controlled pyramidal InGaAs/GaAs quantum dots (QDs) grown by metalorganic vapor phase epitaxy with tailored emission energy and periods as small as $200\,\mathrm{nm}$, suitable for the integration with compact photonic structures. The observed variation of the QD emission energy with the geometric parameters of the array is attributed to adatom and precursor diffusion mechanisms during epitaxial growth. By adjusting the pattern geometry, the emission energy can be tuned over a wide range of $\sim 80\,\mathrm{meV}$ around $1.4\,\mathrm{eV}$, with inhomogeneous broadening $< 10\,\mathrm{meV}$. Single photon emission of isolated QDs with $g^{(2)}_{\mathrm{X,X}}(0) = 0.11$ is demonstrated, which attests to the suitability of these QDs for nanophotonic applications.

Semiconductor quantum dots (QDs) are considered as practical sources of single[1] or entangled[2] photons for integrated quantum photonic chips,[3,4] which incorporate components to generate, route, process and detect[5] quantum states of light.[6] Whereas most preliminary tests of these concepts have been implemented using self-assembled QDs,[5] which do not provide spatial, spectral or polarization control over the emitted photons, this integration would greatly benefit from the development of a scalable QD fabrication platform.[7–9] In particular, the sites of all the QDs should be simultaneously controlled for spatial matching with the modes of the photonic structures,[10–15] be flexible in polarization to match the state of the photonic mode,[16,17] and exhibit reproducible and deterministic emission wavelengths.[18,19] Wavelength control is especially important for tuning the QD emission energy with respect to the photonic mode of interest, in order to achieve significant Purcell or strong coupling effects. In this regard, several methods for a fine, dynamic tuning of the QD energy have been put forward, using, e.g., electric,[20] magnetic[21] or strain fields[22] (occasionally combined[23]) and local temperature variations.[24] However, fixed wavelength setting by direct modification of the QD structure or composition is also useful for adapting the QDs to specific photonic elements on the chip or for on-chip wavelength multiplexing[25] of single photon sources or nanolasers.

Here we report on the deterministic tuning of the emission energy of site-controlled pyramidal InGaAs/GaAs QDs, arranged on triangular arrays with interdot distance as small as $200\,\mathrm{nm}$. These dense arrays[26] are suitable for the insertion of both single QDs[27] and multiple QD systems[12,28] into various photonic integrated structures, for applications such as single photon sources[29] and nanolasers.[30] The wavelength tuning is accomplished by controlling the QD thickness through a systematic variation of the geometric features of the pattern. The growth mechanisms responsible for the observed tuning, particularly the adatom and precursor diffusion processes involved, are discussed. Remarkably, this energy tuning is achieved maintaining a low inhomogeneous broadening ($< 10\,\mathrm{meV}$ near the $1.4\,\mathrm{eV}$ emission energy). Single photon emission from single QDs isolated from the arrays via post growth, selective etching is also demonstrated.

The InGaAs/GaAs QDs were grown on a semi-insulating GaAs (111)B substrate, patterned with $150\,\mu\mathrm{m}$ by $150\,\mu\mathrm{m}$ squares, containing triangular arrays of inverted pyramids with side length s and pitch p.[31] A Scanning Electron Microscope (SEM) image of a $p = 200\,\mathrm{nm}$ array is shown in Fig. 1(a). The selected values of s and p ($\sim 200\,\mathrm{nm}$) are comparable to the diffusion length of the adatoms during the subsequent metalorganic vapor phase epitaxy (MOVPE),[32] hence they influence the thickness and composition of the QDs and their emission wavelength. The growth was performed in a horizontal MOVPE reactor, using N_2 as the carrier gas, and trimethylgallium and arsine as the group III and group V precursors, respectively. The layer stack, deposited at $590\,^{\circ}\mathrm{C}$, consisted in a $3.8\,\mathrm{nm}$ thick GaAs buffer layer (the full set of growth conditions is published elsewhere[31]), followed by a $0.2\,\mathrm{nm}$ thick $In_{0.2}Ga_{0.8}As$ layer. The structure was capped by a $4\,\mathrm{nm}$ thick GaAs layer. All thickness and composition values mentioned are nominal, i.e. determined from calibration growth runs performed under the same conditions on unpatterned GaAs (100) substrates. The Atomic Force Microscopy (AFM) scan of Fig. 1(b) presents the morphology of a pyramid array ($s = 170\,\mathrm{nm}$, $p = 200\,\mathrm{nm}$) overgrown with an $8\,\mathrm{nm}$ thick GaAs layer, to illustrate the evolution of the pattern morphology towards a hexagonal symmetry during growth.[31]

The emission properties of the QD arrays were investigated by low temperature ($10\,\mathrm{K}$) micro-photoluminescence (μPL) measurements performed in a helium-flow cryostat, with $80\,\mu\mathrm{eV}$ spectral resolution. The μPL was excited with a titanium-sapphire laser operating at $730\,\mathrm{nm}$ in continuous wave, focused through a microscope objective (numerical aperture 0.5, spot size $\sim 1\,\mu\mathrm{m}$) onto the sample. The μPL signal was collected through the same objective and dispersed by a grating coupled to a liquid nitrogen cooled Si CCD detector.

The power dependence of the μPL spectrum of a QD array having $s = 170\,\mathrm{nm}$ and $p = 200\,\mathrm{nm}$ is displayed in Fig. 1(c). The number of excited QDs depends on the ratio between

a)Present address: Dipartimento di Fisica, Sapienza Università di Roma, Piazzale A. Moro 1, I-00185 Roma, Italy
b)Electronic mail: eli.kapon@epfl.ch

the spot size and p. The power dependences relative to several $p = 250\,\mathrm{nm}$ arrays with different s are displayed in Fig. 1(d)–(f). At high excitation power, the spectra show a smooth line shape, resulting from the combined effect of the power-dependent broadening of the different excitonic transitions[33] and of the emergence of multiexcitonic states. By decreasing the excitation power, the spectra reveal several narrow lines, corresponding mainly to the neutral and charged excitonic transitions of the probed QDs. These narrow lines attest to the high quality of the QDs grown in such small recesses. The mean emission energy blue shifts for larger s, which suggests that the QD thickness and/or its In content decrease with increasing s. The full width at half maximum (FWHM) of the PL was determined by fitting the low-power spectrum with a Gaussian peak. The obtained values of the FWHM range from $10\,\mathrm{meV}$ for the smaller pyramids ($s = 150\,\mathrm{nm}$) to $7.6\,\mathrm{meV}$ for the larger ones ($s = 200\,\mathrm{nm}$). These values reflect not only the inhomogeneous broadening of the QD ensemble, but include also the separation between the neutral (X) and the negatively charged exciton (X^-), typically $\sim 5\,\mathrm{meV}$.[34]

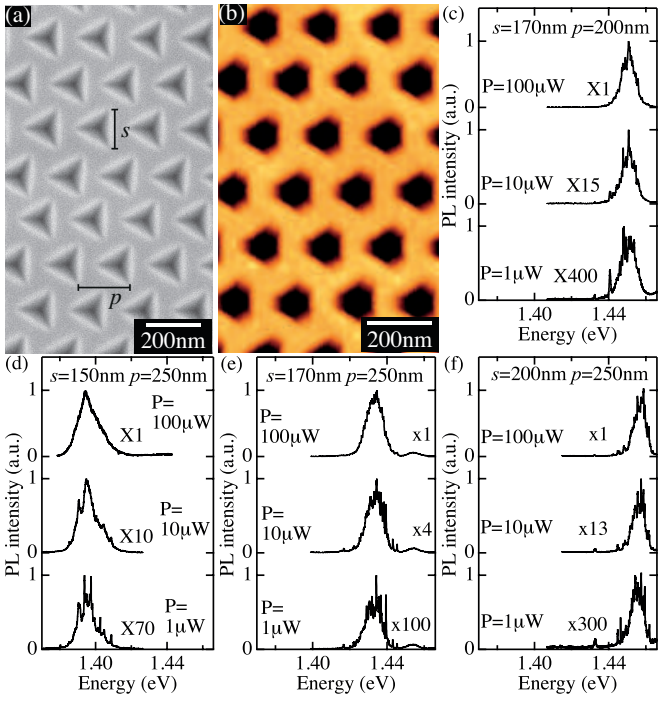

Figure 1. (a) SEM image of a dense array of pyramids ($s = 150\,\mathrm{nm}$, $p = 200\,\mathrm{nm}$). The relevant geometric features are indicated. (b) AFM image of a pyramid array ($s = 170\,\mathrm{nm}$, $p = 200\,\mathrm{nm}$) after MOVPE. Power dependent μPL spectra of QD arrays grown side by side in pyramids having (c) $s = 170\,\mathrm{nm}$, $p = 200\,\mathrm{nm}$ and $p = 250\,\mathrm{nm}$ with (d) $s = 150\,\mathrm{nm}$, (e) $s = 170\,\mathrm{nm}$, and (f) $s = 200\,\mathrm{nm}$.

A study of the uniformity of the PL spectra was performed on a QD array with $s = 200\,\mathrm{nm}$ and $p = 400\,\mathrm{nm}$, grown on the same substrate. μPL spectra were measured every $10\,\mu\mathrm{m}$ at an excitation power of $10\,\mu\mathrm{W}$ across a line parallel to one of the array sides. In Fig. 2(a), three representative spectra measured at a distance of $40\,\mu\mathrm{m}$ to $120\,\mu\mathrm{m}$ from the pattern edge are shown (the spectra have been rescaled to avoid overlap). In Fig. 2(b) we present the central energies of the QD array emission, obtained from Gaussian fits of the μPL spectra. Except for the points at the borders of the pattern, the peak PL energy varies by less than $2\,\mathrm{meV}$ across the $150\,\mu\mathrm{m}$ wide sample, comparable to the inhomogeneous broadening of the excitonic transition measured on similar, isolated QDs.[19] The larger deviations of the QD energy at the borders can be attributed to mass transport of growth species between areas of different local growth rate.[35]

The global trend of the QD emission energy as a function of s and p is summarized in Fig. 2(c), where the peak energies of the QD ensembles measured in the center of the patterns (extracted from Gaussian fits) are displayed for different geometries. The QD PL blue shifts for increasing s. Moreover, the slope of the curves varies similarly for all five p values presented, with a visible slope decrease for $s > 225\,\mathrm{nm}$. AFM measurements performed on a similarly patterned GaAs substrate – on which growth was interrupted right after depositing the $3.8\,\mathrm{nm}$-thick GaAs buffer layer – indicate that the width of the $\{111\}$A planes after growing the buffer is smaller by $15 - 20\,\mathrm{nm}$ than the size s of the as-etched pits (determined via SEM).[31] These measurements also demonstrate that even in the case of very small pyramids, the recess profile attains the self-limited regime,[36] resulting in the same size s_{QD} of the QD formation site for a range of thicknesses of the GaAs buffer.[31] We expect that the majority of the pyramid arrays described here exhibits the same s_{QD}, hence the effects of the non-planarity of the substrate on the effective growth rate should be similar. The observed dependence of the QD emission energy on s is qualitatively explained as follows. The adatom diffusion length, d_{a}, defines an area centered at the pyramid tip, where the exchange of adatoms between the QD (111)B-oriented site and the $\{111\}$A pyramid sidewalls can take place,[37] see Fig. 3(a). The actual growth rate at the pyramid tip depends on the chemical properties of the crystal surfaces comprised within this diffusion area: the adatom incorporation on the $\{111\}$A oriented pyramid sidewalls is indeed twice more likely as compared to the (111)B surface.[38] When the recess size at the moment of QD deposition is larger than the adatom diffusion length, the diffusion area primarily includes favourable incorporation sites. Under these conditions, a chemically driven out diffusion of adatoms occurs, resulting in the partial depletion of the QD layer and hence in a strong blue shift of the QD emission energy for increasing s, as indeed observed for $s < 225\,\mathrm{nm}$. For larger values of s, the adatom diffusion range is likely included inside the pyramids, and the blue shift saturates, as shown in Fig. 2(c). In order to estimate d_{a} from the observed saturation of the QD energy, however, we must consider that the actual size of the recess when the QD is deposited is smaller than the value of s measured for the patterned substrate, due to the gradual filling of the pyramids during the deposition of the buffer layer.

Another characteristic dependence of the PL wavelength is represented by the red shift observed for increasing array pitch p, see Fig. 2(c). This behaviour can be ascribed to the diffusion mechanism of the metalorganic precursors, which have a much larger diffusion length, d_{p}, than that of adatoms (d_{p} is of the order of $\sim 10 - 100\,\mu\mathrm{m}$, as compared to values of d_{a}

of the order of hundreds of nm[32]). These precursors can sample a large number of pyramids in our patterns, as schematically illustrated in Fig. 3(b), only decomposing inside the pyramids.[36] Thus, denser pyramid arrays (smaller p) provide a larger number of decomposition sites for a given precursor diffusion length, which leads to a smaller number of adatoms per QD site and to a blue shift of the QD emission wavelength. The energy of QD arrays with $s = 150\,\mathrm{nm}$ displays, however, an anomalous trend as a function of p. For $p = 400\,\mathrm{nm}$, the expected growth rate is very large (smallest pyramids in the most dilute array). Such a high growth rate results in a strong modification of the shape of the recess, inducing a widening and flattening of the pyramid bottom[31] before the QD layer is deposited. Thus, capillarity effects[39] are reduced on this template, leading to a thinner-than-expected QD layer and to a smoother dependence of the QD emission energy versus s (small red shift from $s = 170\,\mathrm{nm}$ to $s = 150\,\mathrm{nm}$, see Fig. 2(c)). For intermediate values of p ($p = 250$ to $350\,\mathrm{nm}$), the reduction of the growth rate associated with decreasing inter-pyramid distance (i.e., with increasing pyramid density) mitigates the flattening effect described above, capillarity effects are more pronounced, the QDs are thicker and the PL signal red shifts as p is decreased. For $s = 150\,\mathrm{nm}$, $p = 200\,\mathrm{nm}$, the growth rate reduction related to the increasing pyramid density enables us to recover the trend observed for the majority of the patterns, as demonstrated by the significant QD thinning (i.e., blue shift) with respect to the $s = 150\,\mathrm{nm}$, $p = 250\,\mathrm{nm}$ case.

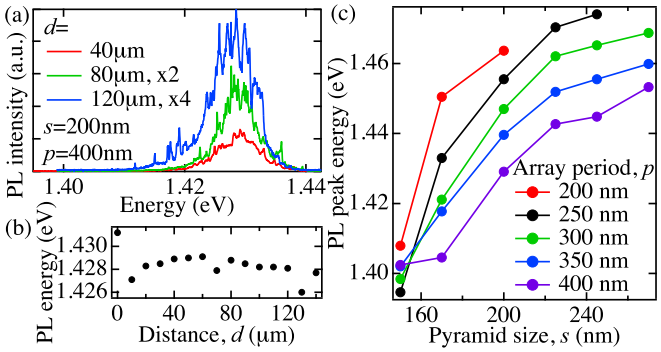

Figure 2. (a) Three μPL spectra (scaled to avoid overlap) acquired at different positions d across the patterned QD arrays. (b) Position dependence of the peak PL energy of the QD ensemble ($s = 200\,\mathrm{nm}$, $p = 400\,\mathrm{nm}$). (c) Variation of peak energy of the QD ensemble versus pyramid size s for different array pitches p.

From the discussion above, it is apparent that the QD thickness and emission wavelength should scale with the areas of the exposed $\{111\}$A and $\{111\}$B surfaces, corresponding to an equilateral triangle of size s and a hexagon of size $p/\sqrt{3}$ minus the area occupied by the $\{111\}$A surface, respectively. In Fig. 3(c) we plot the QD emission energy (central energy of the PL spectrum of the QD ensemble) as a function of $s^2/(2p^2 - s^2)$, which represents the ratio of the $\{111\}$A and $\{111\}$B areas exposed. Remarkably, the curves representing the QDs grown in the largest pyramids ($s = 225$ to $270\,\mathrm{nm} > d_a$) overlap well, in line with the model described above. The increasing deviation from a universal $s^2/(2p^2 - s^2)$ dependence for $s = 200$ and $170\,\mathrm{nm}$ occurs when the adatom diffusion length is comparable to the pyramid size at the moment of the QD deposition. In this case, the presence of the (111)B surface with a lower sticking probability[38] within the diffusion range of adatoms from the pyramid tip tends to reduce the out diffusion of the adatoms. Finally, the non-monotonic energy dependence observed for the smallest pyramids ($s = 150\,\mathrm{nm}$) reflects the more complex behavior of growth in these structures. An adatom diffusion length $\sim 180\,\mathrm{nm}$[32] can be inferred from the observed trends of the energy of the QD emission (i.e., of the QD thickness) on pyramid size, in combination with the results of extensive AFM measurements.[31]

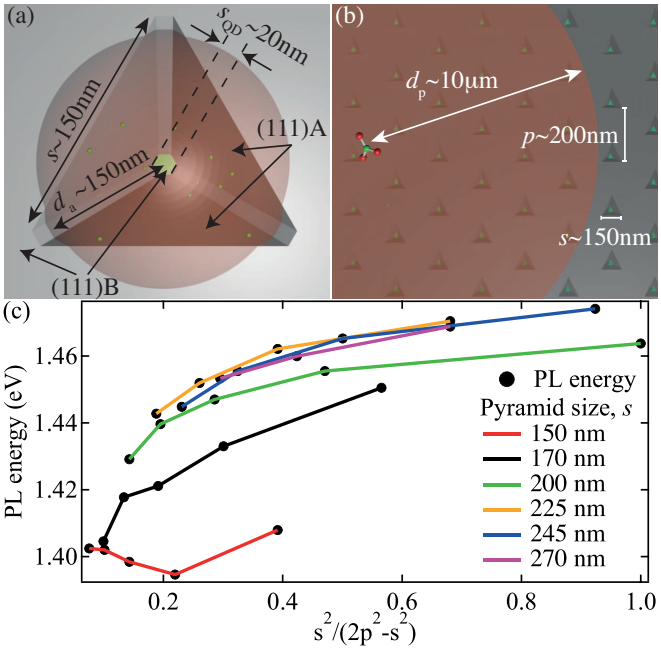

Figure 3. Schematics of the relevant geometric parameters of pyramid arrays as compared with surface diffusion lengths. (a) Adatom diffusion length d_a, much larger than the QD growth site s_{QD} and comparable to the pyramid size s. (b) Metalorganic precursor diffusion length d_p, much larger than the pyramid pitch p. (c) Measured QD emission energy as a function of $s^2/(2p^2 - s^2)$.

We have also investigated the optical properties of single QDs isolated from dense arrays using mesa etching, performed on a sample with $p = 200\,\mathrm{nm}$. The mesas, with diameters ranging from 120 to 150 nm and spacing of 5 μm (see Fig. 4(a)), were fabricated using a standard combination of electron-beam lithography and dry etching.[19] Representative μPL spectra of an isolated pyramidal QD are shown in Fig. 4(b) for several values of the excitation power. At low excitation power, the two main peaks are identified with the negative trion X^- and the neutral exciton X transitions. They are separated by $\sim$ 5 meV, which is the typical value of trion binding energy in these InGaAs/GaAs QDs.[19,34,37] The X linewidth extracted by fitting a Lorentzian curve to the data is 250 μeV, limited at all excitation powers by the effects of fluctuating charged defects at the mesa sidewalls,[40] which are

absent in the case of as-grown QD arrays. At higher excitation power, a third line appears on the high energy side of the X transition, attributed to the biexciton (2X) recombination. A negative 2X–X binding energy has already been observed for pyramidal QDs having comparable transition energies.[34] The second order correlation histogram $g^{(2)}_{\mathrm{X,X}}(\tau)$ shown in Fig. 4(c) was measured using a conventional Hanbury Brown and Twiss setup.[41] The count rate was $> 8000\,\mathrm{counts/s}$, for an overall acquisition of ~ 80 minutes. Pronounced photon antibunching with $g^{(2)}_{\mathrm{X,X}}(0) = 0.11$ (after deconvolution with the instrument response function) was observed, attesting to efficient single photon emission from these QDs.

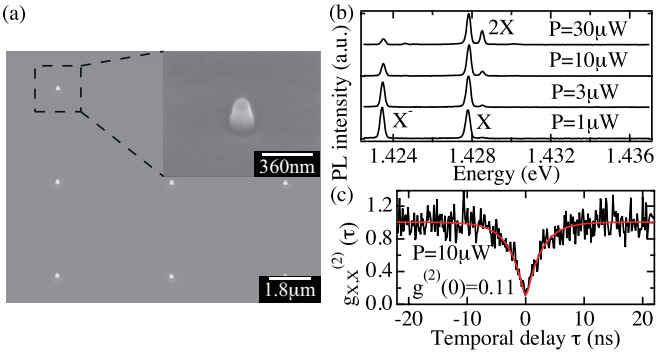

Figure 4. SEM image of an array of mesas, each containing an isolated pyramidal QD. Inset: magnified view of a single mesa. (b) Representative power dependence of the PL spectrum of a single pyramidal QD isolated from a $p = 200\,\mathrm{nm}$ ensemble, measured at $10\,\mathrm{K}$. (c) Autocorrelation histogram of the exciton at $T = 10\,\mathrm{K}$. The red line represents a least squares fitting.

The deterministic fabrication of systems of site-controlled QDs with prescribed emission wavelengths is useful for applications in integrated quantum photonics, where a simultaneous spatial and spectral matching of the light source with the confined optical modes is essential. A high density of QDs is needed when the optical modes exhibit subwavelength features, e.g., in photonic crystal or plasmonic structures, and when high optical gain is required, e.g., in QD-based nanolasers. Producing such QD systems by growth on patterned, non-planar substrates presents challenges both in the stringent requirements it imposes on the spatial resolution of the employed lithographic techniques (array pitch of $\lesssim 200\,\mathrm{nm}$) and in the difficulty of performing epitaxial growth on very shallow features ($\lesssim 100\,\mathrm{nm}$). In particular, the regularity and the quality of such dense arrays of QDs could be compromised due to lithography imperfections, rapid surface planarization during deoxidation, and very thin buffer layers underneath the QDs. In this work we show that it is possible to produce high quality pyramidal InGaAs/GaAs QDs by MOVPE on patterned GaAs (111)B substrates with array pitch as small as $200\,\mathrm{nm}$ and initial pit depths as small as $\sim 120\,\mathrm{nm}$ without compromising the quality of the QDs. The high quality of these nanostructures is attested by their small inhomogeneous broadening, regular excitonic spectral lines, and by the emission of single photons with a high degree of photon antibunching. Moreover, the emission energy of the QD arrays can be adjusted over an $\sim 80\,\mathrm{meV}$ range by appropriately setting the pitch p and the size s of the pyramidal array. A simple epitaxial growth model explains the main wavelength variation trends and enables to tailor the emission energies according to application needs. Such wavelength-tailored site-sontrolled QDs will be useful as a platform for integrated quantum photonic circuits for generating and processing quantum states of light.

ACKNOWLEDGMENTS

This work was supported by the Swiss National Science Foundation.

REFERENCES

[1] P. Michler, A. Kiraz, C. Becher, W. V. Schoenfeld, P. M. Petroff, L. D. Zhang, E. Hu, and A. Imamoğlu, Science **290**, 2282 (2000).
[2] N. Somaschi, V. Giesz, L. De Santis, J. C. Loredo, M. P. Almeida, G. Hornecker, S. L. Portalupi, T. Grange, C. Antón, J. Demory, C. Gómez, I. Sagnes, N. D. Lanzillotti-Kimura, A. Lemaître, A. Auffèves, A. G. White, L. Lanco, and P. Senellart, Nature Photonics **10**, 340 (2016).
[3] E. Murray, D. J. P. Ellis, T. Meany, F. F. Floether, J. P. Lee, J. P. Griffiths, G. A. C. Jones, I. Farrer, D. A. Ritchie, A. J. Bennett, and A. J. Shields, Applied Physics Letters **107**, 171108 (2015).
[4] G. Reithmaier, M. Kaniber, F. Flassig, S. Lichtmannecker, K. Müller, A. Andrejew, J. Vučković, R. Gross, and J. J. Finley, Nano Letters **15**, 5208 (2015).
[5] C. P. Dietrich, A. Fiore, M. G. Thompson, M. Kamp, and S. Höfling, Laser & Photonics Reviews **10**, 870 (2016).
[6] A. J. Shields, Nature Photonics **1**, 215 (2007).
[7] S. Birindelli, M. Felici, J. S. Wildmann, A. Polimeni, M. Capizzi, A. Gerardino, S. Rubini, F. Martelli, A. Rastelli, and R. Trotta, Nano Letters **14**, 1275 (2014).
[8] W. Unrau, D. Quandt, J.-H. Schulze, T. Heindel, T. Germann, O. Hitzemann, A. Strittmatter, S. Reitzenstein, U. Pohl, and D. Bimberg, Applied Physics Letters **101**, 211119 (2012).
[9] M. Strauß, A. Kaganskiy, R. Voigt, P. Schnauber, J.-H. Schulze, S. Rodt, A. Strittmatter, and S. Reitzenstein, Applied Physics Letters **110**, 111101 (2017).
[10] J. Tommila, V. V. Belykh, T. V. Hakkarainen, E. Heinonen, N. N. Sibeldin, A. Schramm, and M. Guina, Applied Physics Letters **104**, 213104 (2014).
[11] T. Hakkarainen, J. Tommila, A. Schramm, J. Simonen, T. Niemi, C. Strelow, T. Kipp, J. Kontio, and M. Guina, Optica **3**, 139 (2016).
[12] A. Surrente, M. Felici, P. Gallo, B. Dwir, A. Rudra, G. Biasiol, L. Sorba, and E. Kapon, Nanotechnology **22**, 465203 (2011).
[13] A. Jamil, J. Skiba-Szymanska, S. Kalliakos, A. Schwagmann, M. B. Ward, Y. Brody, D. J. Ellis, I. Farrer, J. P. Griffiths, G. A. Jones, D. A. Ritchie, and A. J. Shields, Applied Physics Letters **104**, 101108 (2014).
[14] D. Dalacu, K. Mnaymneh, V. Sazonova, P. J. Poole, G. C. Aers, J. Lapointe, R. Cheriton, A. J. SpringThorpe, and R. Williams, Physical Review B **82**, 033301 (2010).
[15] C. Schneider, T. Heindel, A. Huggenberger, T. Niederstrasser, S. Reitzenstein, A. Forchel, S. Höfling, and M. Kamp, Applied Physics Letters **100**, 091108 (2012).
[16] Y.-H. Liao, C.-C. Liao, C.-H. Ku, Y.-C. Chang, S.-J. Cheng, M. Jo, T. Kuroda, T. Mano, M. Abbarchi, and K. Sakoda, Physical Review B **86**, 115323 (2012).
[17] A. Mohan, P. Gallo, M. Felici, B. Dwir, A. Rudra, J. Faist, and E. Kapon, Applied Physics Letters **98**, 253102 (2011).
[18] A. Rastelli, S. Stufler, A. Schliwa, R. Songmuang, C. Manzano, G. Costantini, K. Kern, A. Zrenner, D. Bimberg, and O. G. Schmidt, Physical Review Letters **92**, 166104 (2004).

[19] A. Mohan, P. Gallo, M. Felici, B. Dwir, A. Rudra, J. Faist, and E. Kapon, Small **6**, 1268 (2010).
[20] A. K. Nowak, S. L. Portalupi, V. Giesz, O. Gazzano, C. Dal Savio, P.-F. Braun, K. Karrai, C. Arnold, L. Lanco, I. Sagnes, A. Lemaître, and P. Senellart, Nature Communications **5**, 3240 (2014).
[21] H. Kim, D. Sridharan, T. C. Shen, G. S. Solomon, and E. Waks, Optics Express **19**, 2589 (2011).
[22] S. Sun, H. Kim, G. S. Solomon, and E. Waks, Applied Physics Letters **103**, 151102 (2013).
[23] R. Trotta, E. Zallo, C. Ortix, P. Atkinson, J. D. Plumhof, J. van den Brink, A. Rastelli, and O. G. Schmidt, Physical Review Letters **109**, 147401 (2012).
[24] D. G. Gevaux, A. J. Bennett, R. M. Stevenson, A. J. Shields, P. Atkinson, J. Griffiths, D. Anderson, G. A. C. Jones, and D. A. Ritchie, Applied Physics Letters **88**, 131101 (2006).
[25] A. W. Elshaari, I. E. Zadeh, A. Fognini, M. E. Reimer, D. Dalacu, P. J. Poole, V. Zwiller, and K. D. Jöns, Nature Communications **8**, 379 (2017).
[26] A. Surrente, P. Gallo, M. Felici, B. Dwir, A. Rudra, and E. Kapon, Nanotechnology **20**, 415205 (2009).
[27] C. Jarlov, É. Wodey, A. Lyasota, M. Calic, P. Gallo, B. Dwir, A. Rudra, and E. Kapon, Physical Review Letters **117**, 076801 (2016).
[28] A. Surrente, M. Felici, P. Gallo, B. Dwir, A. Rudra, G. Biasiol, and E. Kapon, Applied Physics Letters **107**, 031106 (2015).
[29] M. H. Baier, E. Pelucchi, E. Kapon, S. Varoutsis, M. Gallart, I. Robert-Philip, and I. Abram, Applied Physics Letters **84**, 648 (2004).
[30] M. Nomura, N. Kumagai, S. Iwamoto, Y. Ota, and Y. Arakawa, Nature Physics **6**, 279 (2010).
[31] A. Surrente, R. Carron, P. Gallo, A. Rudra, B. Dwir, and E. Kapon, Nano Research **9**, 3279 (2016).
[32] S. T. Moroni, V. Dimastrodonato, T.-H. Chung, G. Juska, A. Gocalinska, D. D. Vvedensky, and E. Pelucchi, Journal of Applied Physics **117**, 164313 (2015).
[33] W. Bak, H. Noh, C. Stambaugh, Y. Arakawa, and W. Jhe, Applied Physics Letters **100**, 022105 (2012).
[34] C. Jarlov, P. Gallo, M. Calic, B. Dwir, A. Rudra, and E. Kapon, Applied Physics Letters **101**, 191101 (2012).
[35] S. Watanabe, E. Pelucchi, B. Dwir, M. H. Baier, K. Leifer, and E. Kapon, Applied Physics Letters **84**, 2907 (2004).
[36] E. Pelucchi, V. Dimastrodonato, A. Rudra, K. Leifer, E. Kapon, L. Bethke, P. A. Zestanakis, and D. D. Vvedensky, Physical Review B **83**, 205409 (2011).
[37] M. Felici, P. Gallo, A. Mohan, B. Dwir, A. Rudra, and E. Kapon, Small **5**, 938 (2009).
[38] E. Pelucchi, S. Watanabe, K. Leifer, Q. Zhu, B. Dwir, P. De Los Rios, and E. Kapon, Nano Letters **7**, 1282 (2007).
[39] G. Biasiol and E. Kapon, Physical Review Letters **81**, 2962 (1998).
[40] M. Bayer and A. Forchel, Physical Review B **65**, 041308 (2002).
[41] R. H. Brown and R. Q. Twiss, Nature **177**, 27 (1956).